

Microstructure and properties of K₂O doped superconducting YBa₂Cu₃O_{7-x}

J. TARTAJ, J. F. FERNANDEZ, P. DURAN, C. MOURE
*Instituto de Ceramica y Vidrio (CSIC), Electroceramics Department,
 28500 Arganda del Rey, Madrid, Spain*

K doped YBa₂Cu₃O_x powders have been obtained by incorporating K₂CO₃ to previously coprecipitated amorphous hydroxide mixtures. Synthesis was performed at 900 °C and an orthorhombic 1 2 3 phase was the final product. Sintering of isopressed bars was carried out from 920 to 940 °C. K doping up to 5 at % led to the development of dense bodies with good superconducting behaviour. Oxygen pick-up during the cooling step following sintering was well accomplished despite the high density of the samples. Transition temperatures ≥ 90 K were measured. Doping above that percentage led to samples with lower density values. The presence of non-superconducting phases, such as CuO and a green phase, was very significant, and suppressed the superconducting transition.

1. Introduction

High temperature superconductor ceramics are one of the most exciting materials that became a reality in the last few years. The Y–Ba–Cu–O system has been extensively studied and will be a powerful technological material when some of the problems, which exist at the moment, are addressed.

Superconductivity phenomena depend critically on the oxygen content of sintered ceramics. High density materials are the basis for improvement of both mechanical properties and the critical current. Both high densities and high oxygen contents can be reached only by carefully controlled processes, which sometimes require annealing treatment in oxygen-rich atmospheres. These treatments represent high production costs, and hinder the reliability of final products. In that sense, processes which reduce the steps involved and increase their effectiveness are the way to improve high temperature superconducting ceramic applications.

Doping YBa₂Cu₃O_{7-x} with alkaline metals, specially with K⁺ cations, favours the formation of an orthorhombic phase in a low oxidating atmosphere [1–5]. The substitution of Ba²⁺ cations by K⁺ is made possible by its similar ionic radius [3]. Potassium doped YBa₂Cu₃O_{7-x} ceramics showed a tendency to present orthorhombic *I*-symmetry and lower room temperature resistivity values than the undoped ones under similar oxygen treatment [2]. No influence of K⁺ cation doping on the critical temperature, T_c , was observed. The effect of alkaline cations was related to an improvement of the synthesis process originated by a lowering of the melting point which drives to a higher reactivity and, as a consequence, to better densification.

The high electropositive nature of alkaline metals favours oxygen pick-up from the atmosphere. The high oxidation state increases the valency of copper, and

drives to more oxygen cations with higher Coulombian interaction and a more packaged unit cell lattice.

The orthorhombic–tetragonal transition takes place at higher temperatures when K⁺ is substituted for Ba²⁺ cations [4]. An increase of 100 °C is reached at 10 at % substitution, and the transition takes place at 800 °C; whereas for 20 at %, the transition temperature increases to 825 °C. This increase of the transition temperature allows possible annealing of superconducting ceramics at higher temperatures; which allows better oxygen capture and requires less time. However, no influence of doping levels on the microstructure was reported [4].

From the point of view of the reliability of ceramic processes, it is necessary to understand the influence of doping on both the microstructure and the superconducting properties. The aim of this work is to study the influence of doping YBa₂Cu₃O_{7-x} with K⁺ cations on its sintering behaviour. The relationships between microstructural development and superconductivity properties will also be studied.

2. Experimental procedure

YBa_{2-y}K_yCu₃O_{7-x} ($y = 0.5, 2.5$ and 4 at % K⁺) was prepared by ceramic powder hydroxide coprecipitation route previously reported [6]. The coprecipitated powders were carefully washed prior to chemical analysis by inductively coupled plasma atomic emission spectrometry (ICP–AES), and did not show any traces (< 50 ppm) of precipitant agent, KOH. Then, potassium was added as K₂CO₃ and mixed by ball milling in an isopropyl alcohol medium in a planetary zirconia jar, with posterior drying. The same treatment was performed with the undoped coprecipitated powder, which was taken as a reference material [6].

Synthesis treatment, at different temperatures and times, were performed in alumina crucibles on an electric furnace. The optimum synthesis treatment was 900 °C for 4 h, with a heating rate of 3 °C min⁻¹, and cooling rate of 1 °C min⁻¹. This low cooling rate favours oxygen pick-up and, therefore, the orthorhombic *I*-symmetry can be reached.

The synthesis powders were milled again, and were isostatically pressed at 200 MPa. Sintering treatments were performed in an air atmosphere at 920, 930 and 940 °C with similar schedule rates previously described. The following analyses were performed for characterization of the ceramic materials [6].

X-ray diffraction (XRD) measurement for crystalline phase composition and cell lattice parameters; geometrical determination and Archimedes method for densities; scanning electron microscopy (SEM) with energy dispersive spectroscopy (EDX), and light reflecting optical microscopy (LROM) for microstructural analysis; resistivity measurements versus temperature for T_c determinations have been carried out.

3. Results and discussion

Fig. 1 shows the XRD patterns of both the coprecipitated powder of $\text{YBa}_{1.975}\text{K}_{0.025}\text{Cu}_3\text{O}_{7-x}$ and the calcined one. The coprecipitated powder pattern corresponded to a mixture of amorphous phases, hydroxides of Cu^{2+} and Y^{3+} cations. The presence of $\text{BaCO}_3 \cdot \text{K}_2\text{CO}_3$ was not high enough to be detectable by this technique. After calcining, only one crystalline phase was observed, the 123 orthorhombic *I* crystalline phase, which showed a relation $I_{006}/I_{200} \approx 2$. The lattice parameters of the unit cell were determined in each case (Table I), and corresponded to a well oxygenated $\text{YBa}_{2-y}\text{K}_y\text{Cu}_3\text{O}_{7-x}$ ($7-x \approx 6.95$).

Fig. 2 shows the morphology of the synthesis powders; this consisted of agglomerates of 10–20 μm , con-

TABLE I Lattice parameters of the unit cell of $\text{YBa}_{2-y}\text{K}_y\text{Cu}_3\text{O}_{7-x}$ synthesis powders with different K_2O amounts (nm ± 0.0005)

	<i>a</i>	<i>b</i>	<i>c</i>	7- <i>x</i>
0 at % K_2O	0.3825	0.3891	1.1670	6.96
0.5 at % K_2O	0.3819	0.3884	1.1676	6.93
2.5 at % K_2O	0.3826	0.3890	1.1670	6.96
4.0 at % K_2O	0.3830	0.3890	1.1668	6.97

stituted of small particles, $\approx 2 \mu\text{m}$, with sintered necks between them, which denotes the start of the sintering process.

Fig. 3 shows densification versus temperature curves. The presence of K_2O up to 2.5 at % improves the sintering process, and high densities were reached. Higher K_2O amounts decreased the final density.

At the first stage of sintering density values near 90% D_{th} were reached, and K_2O solid solution in the

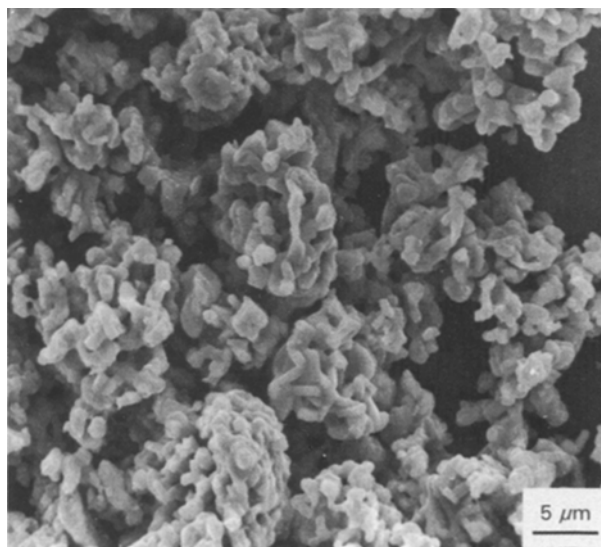


Figure 2 SEM of porous calcined powder.

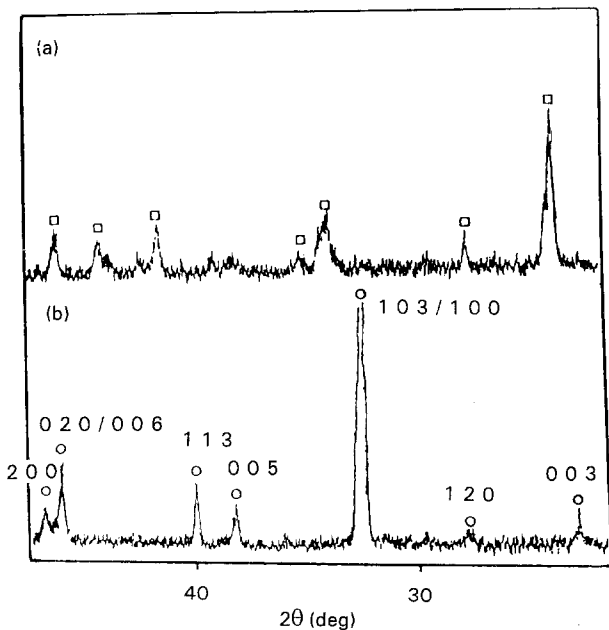


Figure 1 XRD patterns of (a) coprecipitated powder, and (b) synthesized powder: (○) $\text{YBa}_{2-y}\text{K}_y\text{Cu}_3\text{O}_{7-x}$, (□) BaCO_3 .

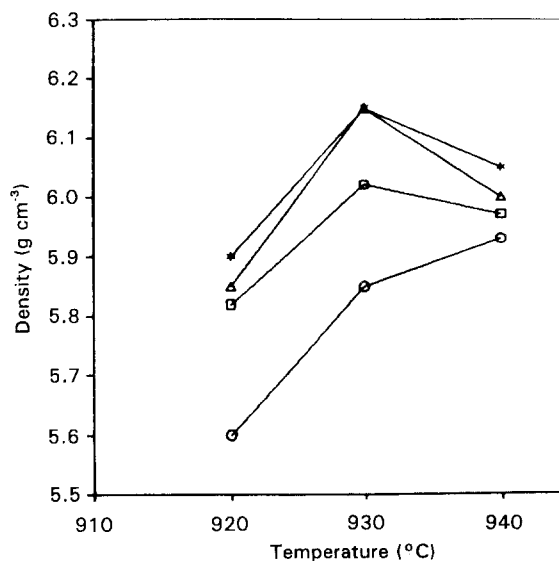
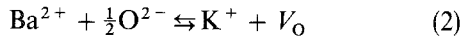
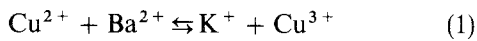


Figure 3 Densification versus sintering temperature for different doped levels.

perovskite lattice can be produced according to the following equations [2]

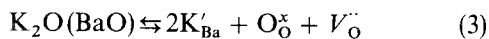


The first equation requires a change in the valency of copper cations, and implies no variation in the oxygen content of the crystalline lattice. In contrast, Equation [2] produces oxygen vacancies and maintains the valency of copper. The second process implies that oxygen is stripped from basal planes (01 positions); which is not energetically favourable because of its previous deficiency in oxygen and high positive charge.

At 930 °C, the density reached a maximum value $\approx 97\% D_{\text{th}}$, for 2.5 at % K_2O . Higher temperatures led to lower densities, probably due to a recrystallization process with rapid grain growth. The presence of 4 at % K_2O in the $\text{YBa}_{2-y}\text{K}_y\text{Cu}_3\text{O}_{7-x}$ doped samples also showed lower densities. Besides a continuous increasing in density, as a function of temperature, could be observed. For this doping level, the solid solution limit was probably exceeded. This means that the appearance of secondary phases retards the sintering process.

Figs 4 and 5 show XRD patterns of the sintered ceramics with 4 and 2.5 at % K_2O , respectively. In the case of the highest doping content, reaction between $\text{YBa}_2\text{Cu}_3\text{O}_{7-x}$ and K_2O takes place at the lowest sintering temperature, and then secondary phases appear. Thus, at 920 °C the symmetry was orthorhombic and copper oxide and green phase, 211, were present. The quantity of secondary phases seems to increase with both time and sintering temperature. CuO also appears and was associated with the lowering of crystalline symmetry.

Lower potassium contents led to the development of pure orthorhombic crystalline phases. In the case of 2.5 at % K_2O , high density ceramics ($\approx 97\% D_{\text{th}}$) at 930 °C (2 h) drive a low oxygen content phase, orthorhombic type II. Higher sintering temperatures and times, 940 °C, 4 and 8 h, gave rise to an enlargement of the [005] and [020]/[006] peaks and the oxygen content reached the highest value, 6.97, after 8 h treatment. None of the previously proposed equations for the incorporation of K^+ in the perovskite lattice cell explain the improvement of the densification process. In this case, the following process could approximately explain such a behaviour: K^+ cations substituted for Ba^{2+} cations, and the appearance of an oxygen vacancy takes place according to the following equation in the Kroger-Vink notation



where K'_{Ba} are K^+ cations in Ba^{2+} cation positions, $\text{O}_{\text{O}}^{\times}$ are interstitial oxygens and $V_{\text{O}}^{\prime\prime}$ is a double ionized oxygen vacancy. These oxygen vacancies could favour the densification process if they are removed towards the grain boundaries, and therefore shrinkage would take place. In that case, posterior incorporation oxygen must be necessary to achieve the correct oxygen content.

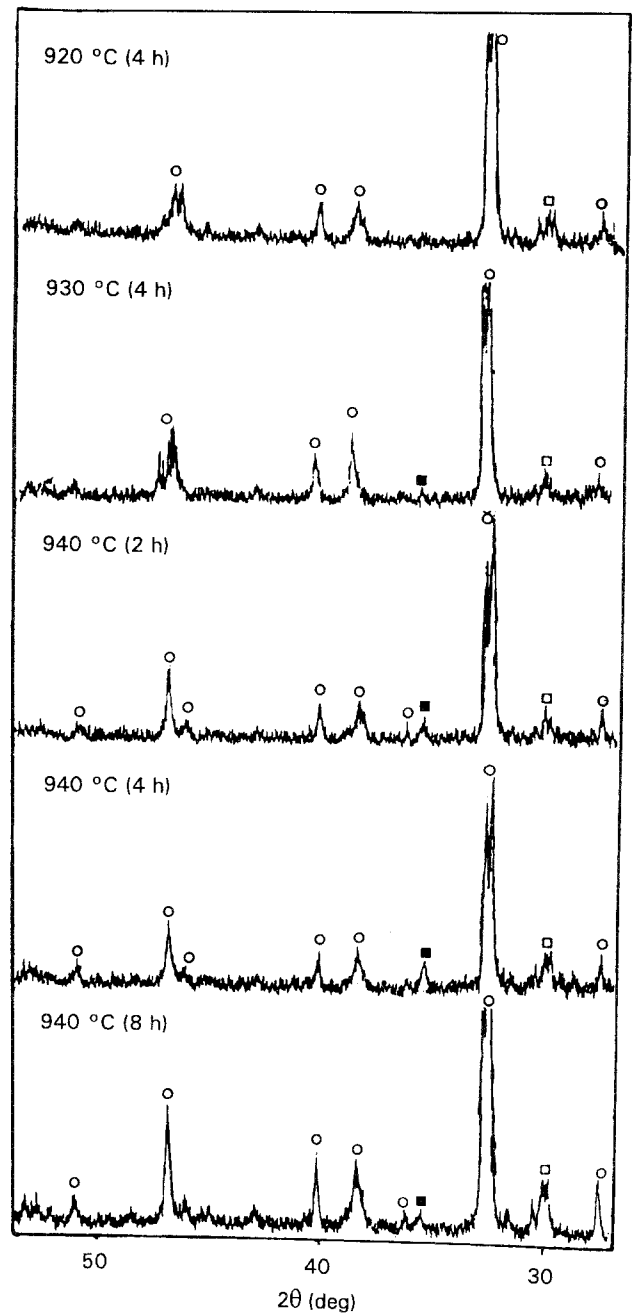
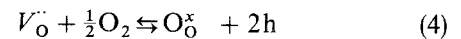


Figure 4 XRD patterns of 4 at % doped sintered samples: (○) $\text{YBa}_{2-y}\text{K}_y\text{Cu}_3\text{O}_{7-x}$ orthorhombic, (□) Y_2BaCuO_5 , (■) CuO .

According to the high oxygen content determined in sintered ceramics, this oxygenation takes place, and the oxygen is responsible for the migration of the oxygen vacancies to the grain boundaries where they are eliminated. The process of oxygenation and annihilation of oxygen vacancies can be described as



which implies a valence change of some copper cations, i.e. Cu^{2+} to Cu^{3+} .

Correlation between the lattice parameters of samples with different K_2O doping levels is not possible due to the different symmetries. However, the similarity of K^+ ionic radii, 0.133 nm, with Ba^{2+} , 0.135 nm, must not produce considerable variation in that parameter. On the other hand, representing the "a" parameter and the orthorhombic distortion as a function of T_c (Fig. 6) a correlation is developed. Both

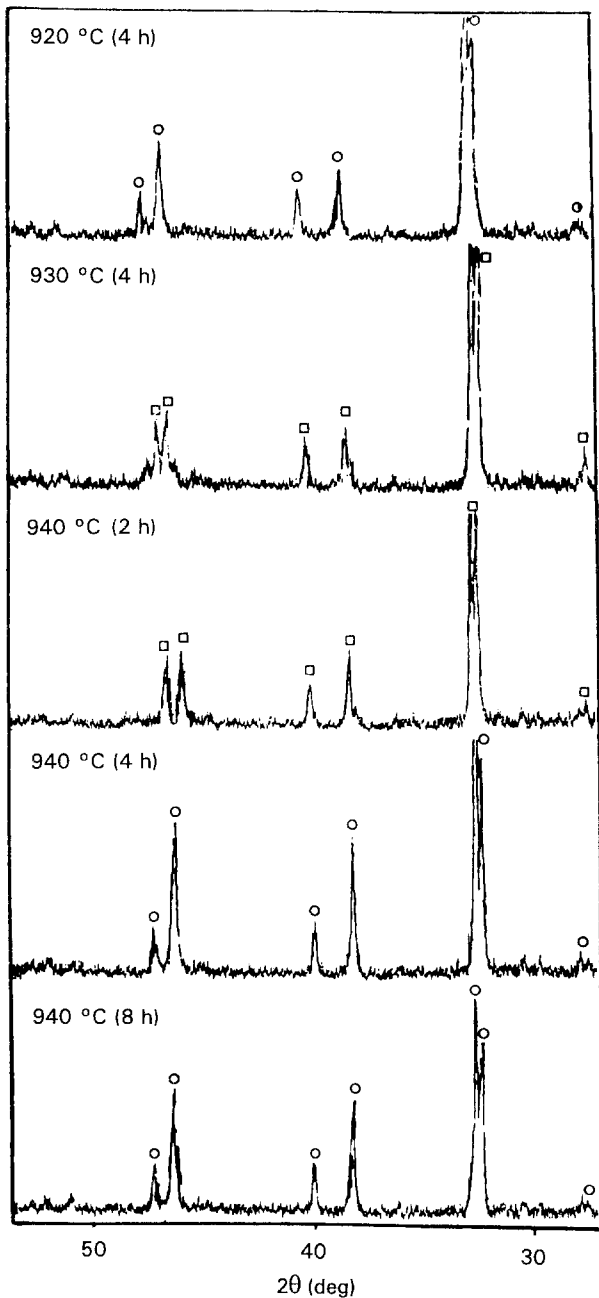


Figure 5 XRD patterns of 2.5 at% doped sintered samples: (○) $\text{YBa}_{2-y}\text{K}_y\text{Cu}_3\text{O}_{7-x}$ orthorhombic, (□) $\text{YBa}_{2-y}\text{K}_y\text{Cu}_3\text{O}_{7-x}$ tetragonal.

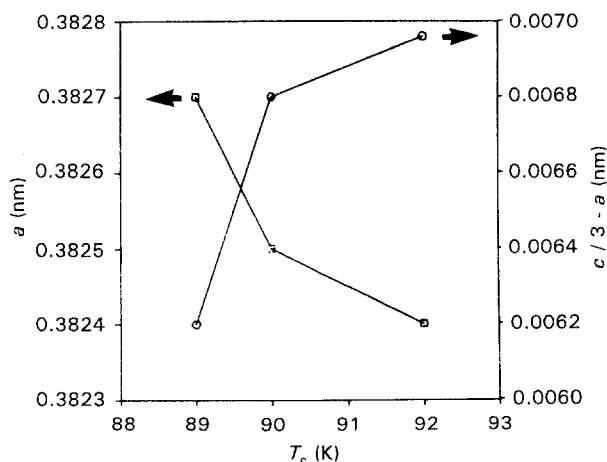


Figure 6 Representation of (○) "a" parameter, and (□) orthorhombic distortion as a function of T_c .

the lowest parameter and the highest orthorhombic distortion leads to the highest critical temperature, and at the same time the transition width is narrowed.

Fig. 7 establishes the relationship between the unit cell volume of the orthorhombic lattice and T_c . The volume of a sample with $T_c = 89$ K was 17.390 nm^3 and that with $T_c = 92$ K was 17.327 nm^3 , that is, there is a decrease of 0.4%. In the same way, the ratio between 006 and 200 peaks showed higher values for higher T_c . Extrapolating both lines, the volume will be 17.34 nm^3 , the ratio I_{006}/I_{200} , will be 3.2 and the temperature, 92.8 K; which represents one of the highest temperatures measured in $\text{YBa}_2\text{Cu}_3\text{O}_{7-x}$ ceramics or, in other words, the most perfect lattice gives the highest T_c .

At this point, it is necessary to remark that the sample which showed a critical temperature at 92 K and a superconducting transition width of 3 K ($\text{YBa}_2\text{Cu}_3\text{O}_{7-x}$ doped with 2.5 at% and sintered at 940°C for 4 h) had the lowest oxygen content, 6.89, in comparison with others which ranged between 6.97 and 6.99. Understanding such behaviour requires a decrease of the cationic charge, K^+ cations for Ba^{2+} cations, which allows the development of ceramic superconductors with a lower oxygen content than the theoretical one of the orthorhombic cell. If the position of Ba^{2+} and K^+ cations and the high orthorhombic distortion are taken into account, this implies that movement of oxygen from 02 or 03 positions in planes to chains in 04 positions could take place. In this case, a higher amount of Cu^{3+} could be generated.

The level of doping for the studied sample, did not reveal a clear influence with the exception of samples doped with 4 at% K_2O , in which the limit of solid solution was exceeded. As a consequence, the influence of potassium doping must be related to microstructural effects which modified the system in a wider manner than the lattice variation could reveal.

Fig. 8 shows the microstructure of 2.5 at% K_2O doped samples at different sintering temperatures and times. The samples sintered at the lowest temperature showed small grain size, and had some bigger grains,

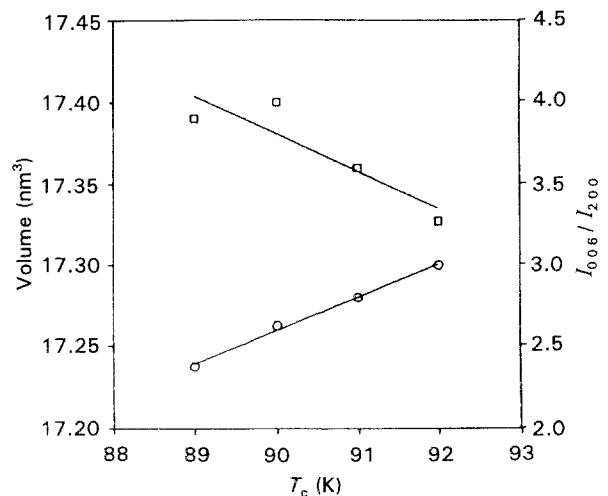


Figure 7 Relation between unit cell volume, T_c and the ratio I_{006}/I_{200} : (○) I , (□) V .

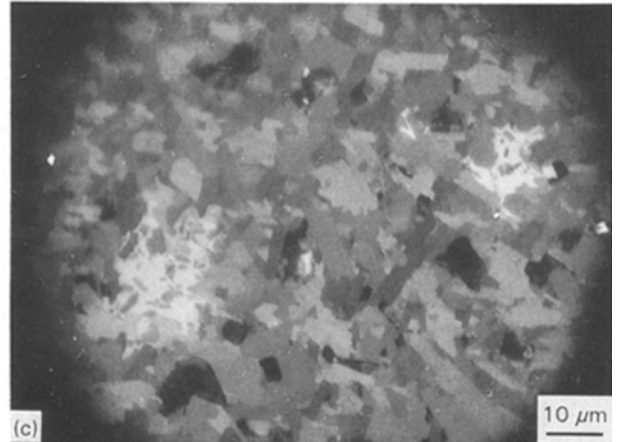
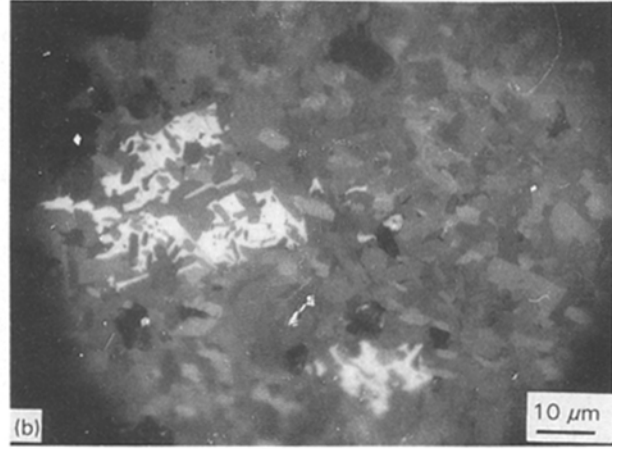
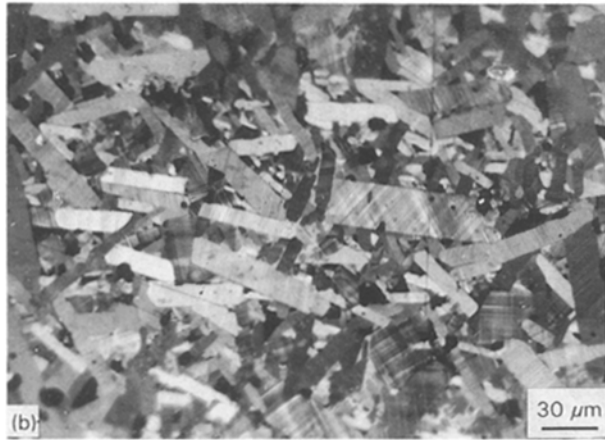
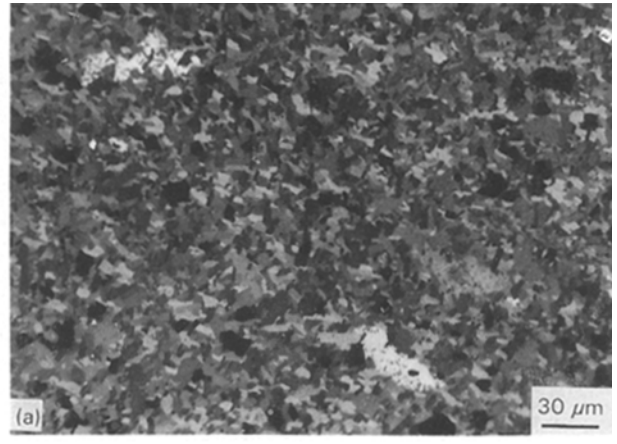


Figure 8 Light polarized optical micrographs of $\text{YBa}_{2-y}\text{K}_y\text{Cu}_3\text{O}_{7-x}$ doped with 2.5 at % K_2O : (a) 920 °C, 4 h; (b) 940 °C, 4 h; and (c) 940 °C, 8 h.

Figure 9 Light polarized optical micrographs of $\text{YBa}_{2-y}\text{K}_y\text{Cu}_3\text{O}_{7-x}$ doped with 4 at % K_2O : (a) 920 °C, 4 h; (b) 940 °C, 4 h; and (c) 940 °C, 8 h.

$\approx 70 \times 30 \mu\text{m}^2$. The increasing of both the temperature and the time of the sintering process enlarged both the small and large grains. In the latter case, the exaggerated grains seem to show a tendency to enlarge more in length than in width. The presence of porosity in the grains revealed that the sintering process rate is higher than the migration of porosity to the grain boundaries. Secondary phases have not been observed from this technique.

On the other hand, 4 at % doped $\text{YBa}_2\text{Cu}_3\text{O}_{7-x}$ showed a very different microstructural development (Fig. 9), without exaggerated grain growth and with the presence of liquid phases; both originated because

solid solution was exceeded. The location of the liquid phase was heterogeneous, corresponding to microfluctuations in the potassium content. According to studies realized by Nae-Li Wu *et al.* [7], the regions with smaller grain size correspond with a higher potassium concentration.

The sample doped with 2.5 at % K_2O shows a microstructure very similar to the undoped one. The microstructure of such a sample was also examined by SEM (Fig. 10). In this case, all the superconducting $\text{YBa}_2\text{Cu}_3\text{O}_{7-x}$ grain boundaries contain a thin layer which was analysed by EDX and contained mainly Ba and Cu [6]. This eutectic liquid was formed from the

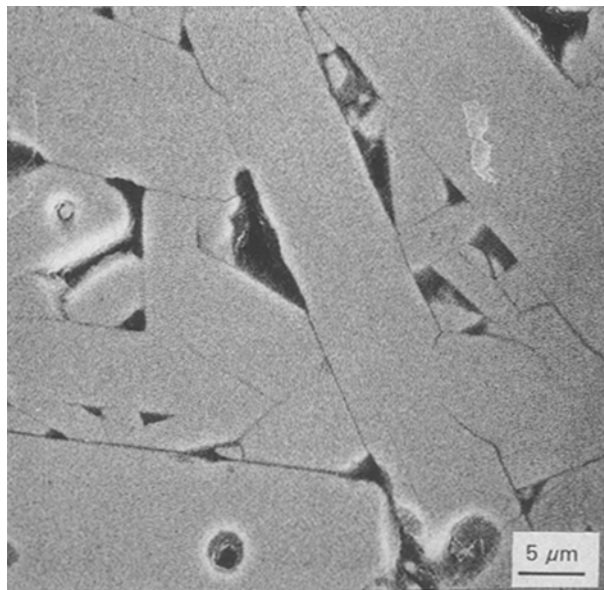
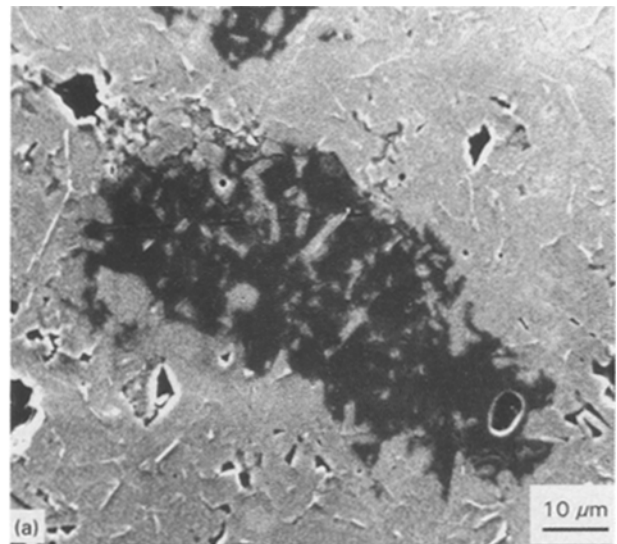


Figure 10 SEM of $\text{YBa}_{2-y}\text{K}_y\text{Cu}_3\text{O}_{7-x}$ sintered samples (2.5 at % K_2O) showing grain boundary liquid thin layer.



BaCO_3 – CuO system at low temperature. These results are similar to those obtained for doped samples up to 2.5 at % K_2O .

Fig. 11a shows a liquid-rich region of sample doped with 4 at % K_2O . The EDX spectra of this liquid phase revealed that it mainly contains CuO (Fig. 11b).

Excess potassium favours the appearance of a non-superconducting green phase, 211, and CuO . This reaction normally occurs at 1015°C in undoped $\text{YBa}_2\text{Cu}_3\text{O}_{7-x}$ [8]. During the cooling step the crystallization rate of the 123 phase from the melt, is higher than the rate of peritectic reaction between the 211 phase and the liquid. This allows the presence of small amounts of 211 phase, and inclusion of CuO grains in 123 phase grains.

4. Conclusions

$\text{YBa}_2\text{Cu}_3\text{O}_{7-x}$ superconducting ceramics have been doped with K^+ cations in the range 0–4 at %, and the solid solution limit was established at ~ 2.5 at %.

The presence of excess K_2O in YBaCuO materials causes the appearance of secondary phases, which are pernicious for superconducting features of such materials, leading to the disappearance of the superconducting transition. The secondary phases are Y_2BaCuO_5 (green phase) and CuO , which remain as vitreous phases according to the microstructural and micro-analytical measurements performed. Moreover, their densities are lower than those of the undoped samples. This feature allows better oxygen pick-up processes and, therefore, leads to the formation of an orthorhombic I crystalline symmetry. Nevertheless, the overall properties of overdoped samples are lower than those corresponding to the undoped ones.

When the amount of K_2O lies below the solid solution limit (≈ 2.5 at % with respect to the Ba

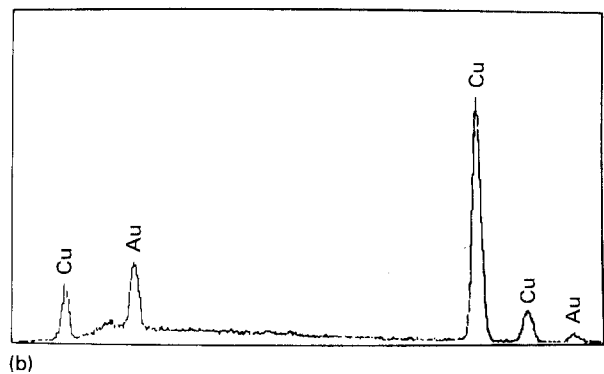


Figure 11 (a) SEM of $\text{YBa}_{2-y}\text{K}_y\text{Cu}_3\text{O}_{7-x}$ sintered samples (4 at % K_2O) showing liquid phase. (b) EDX spectra of this liquid phase.

content), it is possible to obtain denser superconducting materials. Formation of oxygen vacancies, according to the reaction $\text{K}_2\text{O}(\text{BaO}) \rightleftharpoons 2\text{K}'_{\text{Ba}} + \text{O}^{\times}_\text{O} + V^{\bullet\bullet}_\text{O}$, and their subsequent annihilation following the sequence $V^{\bullet\bullet}_\text{O} + 1/2\text{O}_2 \rightleftharpoons \text{O}^{\times}_\text{O} + 2\text{h}^{\bullet}$ could be the cause of the density increases. At the same time, a small percentage of Cu^{2+} changes to Cu^{3+} , which favours the superconducting features. This hypothesis is supported by the high T_c values (≥ 90 K) shown by samples which have oxygen contents as low as 6.85. The higher electropositive character of K^+ with respect to Ba^{2+} could also contribute to improved oxygenation of dense samples.

Acknowledgements

This work was supported by the Comisión Interministerial de Ciencia y Tecnología (MAT88-0219) and by a grant of RHÔNE POULENC QUÍMICA S.A.

References

1. I. FELNER, M. KOWITT and Y. YESHURUN, *Phys. Rev. B.* **36** (1987) 39233.

2. I. W. CHEN, S. KEATING, C. Y. KEATING, X. WU, J. XU, P. E. REYES-MOREL and T. Y. TIEN, *Adv. Ceram. Mater.* **2** (1987) 457.
3. R. D. SHANNON, *Acta. Cryst.* **A32** (1976) 751.
4. I. KONTOULIS, X. TURRILLAS, R. MEISELS, S. BUNGRE and B. C. H. STEELE, *J. Less-Com. Met.* **150** (1989) 139.
5. Y. KHAN, *J. Mater. Sci. Lett.* **7** (1988) 53.
6. J. TARTAJ, C. MOURE, P. DURAN, J. L. GARCIA-FIERRO and J. COLINO, *J. Mater. Sci.* **26** (1991) 6135.
7. N. L. WU, E. RUCKENSTEIN, L. Q. WANG and P. MATTOCKS, *Mater. Lett.* **6(7)** (1988) 211.
8. E. SAIZ, R. TORRECILLAS, S. AZA and J. S. MOYA, in "Superconducting Ceramics", British Ceramics Proceedings, Vol. 40, edited by R. Feer, (Institute of Ceramics, Stoke-on-Trent, 1988) p. 231.

*Received 11 May 1993
and accepted 19 January 1994*